

## Piezoresistance and the conduction-band minima of GaAs

D. E. Aspnes\*

*Max-Planck-Institut für Festkörperforschung, 7000 Stuttgart 80, Federal Republic of Germany  
and Bell Laboratories, Murray Hill, New Jersey 07974 †*

Manuel Cardona

*Max-Planck-Institut für Festkörperforschung, 7000 Stuttgart 80, Federal Republic of Germany  
(Received 10 June 1977)*

Linear (low-stress) and superlinear (high-stress) piezoresistance data are reported for lightly, moderately, and degenerately doped  $n$ -type GaAs single-crystal samples for hydrostatic pressure and for [100] and [111] uniaxial stress. The theoretical expression for mobility for polar-optical scattering predicts a hydrostatic piezoresistance coefficient only half as great as observed, if all pressure-dependent terms in addition to the effective mass are included. If only the mass dependency is retained, agreement is restored and the stress-induced anisotropy of the linear piezoresistance can be explained in terms of the stress dependence of the mass tensor derived in a previous paper. The anisotropy produces different rates of increase of the linear piezoresistance, which in extrapolated relative values at 10-kbar uniaxial (10/3-kbar hydrostatic) stress are  $0 \pm 0.5\%$ ,  $3.4 \pm 0.5\%$ , and  $4.0 \pm 0.5\%$  for [100] uniaxial, hydrostatic, and [111] uniaxial stress, respectively. The superlinear resistance increase observed for [111] uniaxial stress shows that the  $L_1^C$  minima are  $330 \pm 40$  meV above the  $\Gamma_1^C$  minimum, in agreement within experimental uncertainty with the recent stress work of Pickering and Adams and the synchrotron-radiation electroreflectance results of Aspnes, Olson, and Lynch. A shear deformation potential of  $19.6 \pm 3$  eV is obtained. Superlinear resistance increases for [100] stress can be interpreted similarly. However, the anomalously large shear deformation potentials so obtained suggest another origin, possibly electron trapping in point defects or mechanical failure due to incipient fracture, for this effect in [100] stress.

### I. INTRODUCTION

After good single-crystal material became available, thermopower,<sup>1</sup> mass anisotropy,<sup>2-4</sup> and effective-mass<sup>5,6</sup> measurements established that GaAs was a direct-band-gap material with the lowest conduction-band minima at  $\Gamma_1^C$ , the center of the Brillouin zone. The existence of subsidiary minima a few tenths of an eV above  $\Gamma_1^C$  was established even earlier by extrapolating indirect-absorption-edge data on GaAs<sub>1-x</sub>P<sub>x</sub> alloys<sup>7,8</sup> and by measuring the Hall coefficient of GaAs at high temperatures.<sup>9-11</sup> These indirect minima were initially assigned to  $L_1^C$ , on the basis of the first band-structure calculation for GaAs by Callaway.<sup>12</sup>

The first GaAs high-pressure transport data<sup>13</sup> showed the existence of indirect minima 0.5 eV above  $\Gamma_1^C$ . By comparing the pressure coefficient of this threshold to previous work on Si,<sup>14,15</sup> it was clear that these minima had  $X_1^C$  symmetry. Although for a brief time a  $\Gamma$ - $L$ - $X$  ordering remarkably similar to the current self-consistent model<sup>16</sup> was considered,<sup>17</sup> the definitive symmetry assignment, together with the relatively large uncertainties in energy values, acted primarily to cast considerable doubt on the previous  $L_1^C$  interpretation of the alloy<sup>7</sup> and high-temperature Hall-effect<sup>9,10</sup> data. In a comprehensive reexamination, Ehrenreich<sup>18</sup> showed that all existing data were in fact consistent to within experimental error with a model where the  $X_1^C$  indirect minima were

0.36 eV above the absolute  $\Gamma_1^C$  minimum and the  $L_1^C$  minima were sufficiently high in energy to be ignored.

Ehrenreich's  $\Gamma$ - $X$  proposal was so well argued that for the next 16 years the validity of the model itself was not seriously questioned but in fact apparently supported by new or more refined experiments,<sup>19-29</sup> even though adjustments in values (and a contradiction between the optical<sup>22,28</sup> and photoemission<sup>23</sup> data) for the  $X_1^C$ - $\Gamma_1^C$  separation energy were to be found in the accumulating data. Because band structure calculations predicted either an  $L_1^C$  assignment<sup>12,30,31</sup> or an  $X_1^C$  assignment<sup>32,33</sup> for the first indirect threshold, depending upon the method used, and because no local-potential calculation scheme consistently achieved better than 0.5-eV accuracy in other, known situations, band structure calculations did not provide useful information with respect to this problem. For example, first-principles self-consistent orthogonalized-plane-wave calculations<sup>34</sup> yielded  $X_1^C$  minima either 1 eV above or 0.5 eV below  $\Gamma_1^C$ , depending upon whether a Slater or Kohn-Sham exchange was used. Although recent nonlocal pseudopotential calculations<sup>35,36</sup> that provided highly accurate ( $\sim 80$  meV maximum deviation) fits to electroreflectance<sup>37</sup> and photoemission<sup>38,39</sup> data both predicted  $L_1^C$  minima 150–200 meV below  $X_1^C$  (compared to the current experimental value of  $170 \pm 30$  meV) the generally poor record of previous calculations on this scale of energy caused these

predictions not to be taken seriously.

Within the last year, the GaAs band structure was reinterpreted with  $L_1^C$  placed  $170 \pm 30$  meV below  $X_1^C$  on the basis of Schottky-barrier electroreflectance data<sup>40</sup> from the Ga-3d core levels measured in the synchrotron energy range of 20 eV. Using these new data, a comprehensive model was developed<sup>16,41</sup> that placed the  $L_1^C$  and  $X_1^C$  minima 285 and 476 meV, respectively, above the  $\Gamma_1^C$  absolute minimum at 300 K. This model explained a wide range of optical, transport, and band structure data, and resolved previous contradictions between transport and optical data. It was qualitatively supported by threshold velocity and velocity-field characteristics for Gunn oscillators, both measured and calculated, as a function of hydrostatic pressure and uniaxial stress.<sup>42,43</sup> Quantitative support came from luminescence measurements on  $\text{Ga}_{1-x}\text{Al}_x\text{As}$  alloys<sup>44</sup> and from resonant Raman scattering.<sup>45</sup>

Remaining conflicts now concern only uniaxial stress piezoresistance and Gunn oscillator threshold data,<sup>19,24</sup> which seemingly confirmed that the  $L_1^C$  minima lay above  $X_1^C$ . However, these experiments have recently been contested<sup>42,43</sup> as having been performed with poorly defined stress configurations. A "pancake" sample stressed between pressure anvils<sup>19,24</sup> could be expected to undergo significant hydrostatic stress due to confinement in addition to the intended uniaxial stress. The experiments of Ref. 43, with an improved cubical sample geometry, indeed showed that the  $L_1^C$  minima were below  $X_1^C$  but that the separation was very slight ( $\sim 0.02$  eV), in contrast to the comprehensive model and the optical data for the location of  $X_1^C$ .

In view of the discrepancies between the stress data and the results of other experiments, and of the inconsistencies in the stress work, we have performed piezoresistance measurements on *n*-type GaAs using bar-shaped samples to achieve well-defined stress and current configurations. Lightly, moderately, and degenerately doped material was investigated with [100] and [111] uniaxial stress and with hydrostatic pressure.

Our results are as follows. Low-stress (linear-piezoresistance) regime:

(i) We compare the observed resistance change with hydrostatic stress for shallow-donor-dominated samples with the theoretical expression for mobility for polar-optical scattering.<sup>46</sup> The theoretical prediction is low by a factor of two if the measured pressure dependences of all pressure-varying quantities are used to evaluate the change of mobility with pressure. Agreement within experimental accuracy is obtained if only the pressure dependence of the mass, as  $(m^*)^{-1}$ , is as-

sumed.

(ii) We observe a significant low-stress (linear-piezoresistance) anisotropy for shallow-donor-dominated samples. Extrapolated to 10-kbar values, the linear piezoresistance for [100] stress is small,  $0.0 \pm 0.5\%$ , while those for hydrostatic pressure and [111] stress are larger:  $3.4 \pm 0.5\%$  and  $4.0 \pm 0.5\%$ , respectively. These results, surprisingly not observed in previous piezoresistance work, are completely explained by the theory of stress-induced anisotropy of the conduction-band effective mass described in a previous paper.<sup>47</sup>

High-stress (superlinear-piezoresistance) regime:

(iii) We observe the piezoresistance to increase superlinearly for [111] stress  $\chi > 5$  kbar. Analysis of this increase shows that the  $L_1^C$  minima are located  $330 \pm 40$  meV above the  $\Gamma_1^C$  minimum. This is in agreement with the stress results of Pickering and Adams<sup>43</sup> who obtained a  $L_1^C$ - $\Gamma_1^C$  separation of  $300 \pm 30$  meV, and with the comprehensive model,<sup>16</sup> for which the separation is  $285 \pm 30$  meV. The  $L_1^C$  shear deformation potential,  $\mathcal{E}_2^L = 19.6 \pm 3$  eV, deduced from these data is equal to that obtained by Pickering and Adams if an improved value<sup>48</sup> for the hydrostatic contribution to  $\Gamma_1^C$  is used in their calculation. These values are in acceptable agreement with that of  $16.2 \pm 0.4$  eV obtained by Balslev<sup>49</sup> for Ge, and that of  $16.2 \pm 3.5$  eV obtained by Walton and Metcalfe<sup>50</sup> for GaSb.

(iv) We observe a remarkably large superlinear increase in the piezoresistance for [100] stress  $\chi > 6$  or 7 kbar. Assuming this to be due to carrier transfer to  $X_1^C$  [100], we calculate a zero-stress  $X_1^C$ - $\Gamma_1^C$  energy separation of the order of 400–500 meV, in qualitative agreement with the comprehensive model<sup>16</sup> but somewhat larger than the  $330 \pm 70$ -meV value found by Pickering and Adams.<sup>43</sup> The data also predict a shear deformation potential  $\mathcal{E}_2^X$  of the order of 20–30 eV, in essential agreement with that previously measured by Harris, Moll, and Pearson<sup>24</sup> and Pickering and Adams.<sup>43</sup> But these values for  $\mathcal{E}_2^X$  are far larger than those determined by optical measurements on similar materials, which are  $8.6 \pm 0.2$  eV for Si,<sup>49</sup>  $5.4 \pm 0.3$  eV for AlSb,<sup>51</sup> and  $6.9 \pm 0.7$  eV for GaP.<sup>52</sup> Also, we have estimated the shear deformation potential from pseudopotential theory and have found that  $\mathcal{E}_2^X$  should be of the order of 6.3 eV. Because of the wide disagreement between the GaAs piezoresistance and other values for  $\mathcal{E}_2^X$ , we believe another mechanism must be used to explain the apparent carrier transfer results. The generally unreproducible data and the appearance of strong superlinear piezoresistance only within 2 kbar of fracture in our samples suggest that the resistance increase may be due to incipient me-

chanical failure, or possibly to electron trapping in impurity levels, but the same issue cannot be considered closed.

The outline of the paper is as follows. Experimental details and results are summarized in Sec. II. The connection between resistance and intrinsic sample parameters, the linear piezoresistance results, the superlinear piezoresistance results, and the lightly doped sample results are discussed in Secs. IIIA–IIID, respectively.

## II. EXPERIMENTAL

### A. Techniques

Resistance versus uniaxial-stress measurements were taken on *n*-type GaAs single-crystal samples cut to approximate dimensions  $1.5 \times 1.5 \times 15$  mm, with the long dimension parallel ( $\pm 0.5^\circ$ ) to either a  $\langle 100 \rangle$  or  $\langle 111 \rangle$  axis. Three different *n*-type boules were used as source material, with carrier concentrations of  $3 \times 10^{15}$ ,  $7 \times 10^{16}$ , and  $3.8 \times 10^{18}$   $\text{cm}^{-3}$ , respectively. Because it is important to know the carrier concentration and the compensation of these samples, Hall and resistivity measurements were taken from 10 or 77 K to 330 K on these materials. The room-temperature electrical properties of the lightly doped sample were found to be dominated by a shallow trap 210 meV below the conduction-band edge, where  $N_T \approx 6.5 \times 10^{16}$   $\text{cm}^{-3}$ . It is not surprising to find electron traps near this depth in this concentration range in bulk GaAs, although these traps are usually quite sample dependent.<sup>53</sup> The carrier concentration of the medium-doped and heavily doped samples was independent of temperature.

Uniaxial stress was applied by means of the technique previously described.<sup>54–56</sup> With approximate cross-sectional areas of 2.5  $\text{mm}^2$ , the apparatus was capable of producing stresses of over 10 kbar. This value was not reached with  $\langle 100 \rangle$  samples, which always fractured before 8 kbar. Hydrostatic stress measurements were taken to 4 kbar (measured hydrostatic pressure) using a commercial hydraulic apparatus.<sup>57</sup> In all cases, stress was applied slowly to avoid shock. Sufficient time was allowed with hydrostatic stress to permit thermal transients to decay after changing the stress. On the  $[111]$  uniaxial stress samples, some hysteresis ( $< 10\%$ ) was observed upon unloading, which was attributed to relaxation effects in the stress apparatus.

Resistance was determined by a four-point method, where the current was passed through the sample by means of two alloyed Ohmic contacts 8 mm apart, symmetrically located on one side about the midpoint of the bar. The relative resistance was determined by maintaining the current at a constant value and using a high-im-

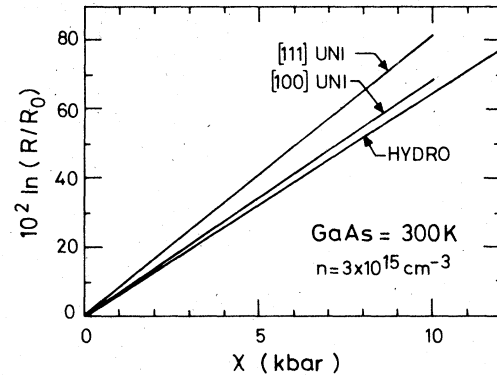


FIG. 1. Dependence of the relative-resistance change  $\Delta R/R$  on stress for lightly doped representative GaAs samples with zero-stress electron concentrations of  $3 \times 10^{15}$   $\text{cm}^{-3}$ .

pedance digital voltmeter to measure the voltage across two similar contacts 3 mm apart symmetrically located on the opposite side of the bar.

### B. Results

Representative results are given in Figs. 1, 2, and 3 for lightly, moderately, and heavily doped GaAs samples. The hydrostatic pressure is actually three smaller than the nominal values given in the figures so as to represent the hydrostatic component applied uniaxially. The lightly doped samples showed large resistance changes because their carrier concentrations were dominated by a deep trap. The much smaller changes observed for the moderately and degenerately doped samples are more representative of intrinsic piezoresistance effects. We place the most emphasis on the results obtained with the moderately doped crystal, for which the hydrostatic-pressure data are in excellent agreement with previous measurements by Sagar<sup>58</sup> on  $8 \times 10^{16}$   $\text{cm}^{-3}$  *n*-type material, and by Pitt and Lees<sup>26</sup> on high-quality liquid-phase

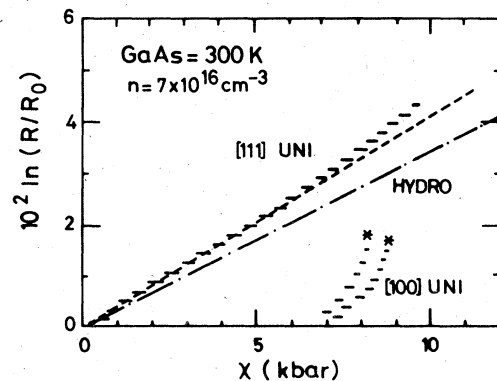


FIG. 2. As Fig. 1, but for moderately doped samples with electron concentrations of  $7 \times 10^{16}$   $\text{cm}^{-3}$ .

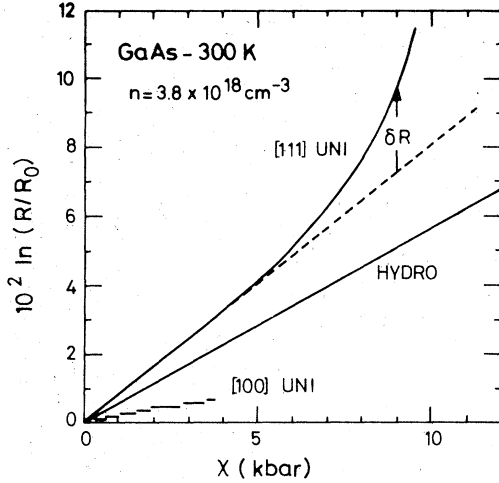


FIG. 3. As Fig. 1, but for degenerately doped samples with electron concentrations of  $3.8 \times 10^{18} \text{ cm}^{-3}$ .

epitaxial material.

The data show several systematics. The low-stress linear piezoresistance regions in the moderately and degenerately doped samples correspond to linear stress-induced changes in the band structure and scattering lifetimes. For all samples, the linear piezoresistance  $R$  increased more rapidly for [111] stress than for [100] stress, and for all but the lightly doped samples the hydrostatic piezoresistance falls between. For large stress, the superlinear resistance component increases more rapidly for the degenerately doped samples, because carrier transfer to the low-mobility indirect minima occurs at lower stresses due to the higher Fermi level in these samples. Samples fractured much more easily with [100] stress than with [111] stress. This is reasonable

TABLE I. Calculated or measured stress-induced changes in parameters determining resistance changes measured in this experiment.

	Hydrostatic $\chi = \frac{10}{3}$ kbar	[100] uniaxial $\chi = 10$ kbar	[111] uniaxial $\chi = 10$ kbar
$\Delta l/l$	-0.00139 <sup>a</sup>	-0.01264 <sup>a</sup>	-0.00759 <sup>a</sup>
$\Delta A/A$	-0.00278 <sup>a</sup>	0.008468 <sup>a</sup>	0.00342 <sup>a</sup>
$\Delta m_c^*/m_c^*$	0.0233 <sup>b</sup>	...	...
$\Delta e^*/e^*$	-0.00190 <sup>c</sup>	...	...
$\Delta \omega_0/\omega_0$	0.00495 <sup>c</sup>	...	...
$\Delta \theta/\theta$	0.00495	...	...
$\Delta R/R$	0.0340 <sup>d</sup>	0.000 <sup>e</sup>	0.041 <sup>e</sup>
$\Delta R/R_{\text{calc}}$	0.0150 <sup>e</sup>	...	...

<sup>a</sup> Calculated from compliance data, Ref. 63.

<sup>b</sup> Magnetophonon data, Ref. 62.

<sup>c</sup> Raman scattering, Ref. 61.

<sup>d</sup> This paper, Fig. 2; also Refs. 26 and 58.

<sup>e</sup> This paper, Fig. 2.

because the dimensional changes are about twice as large for a given [100] stress than for the same [111] stress (see Table I), and thus the effect of point defects in the crystal lattice should be more pronounced in the [100] stress case.

### III. DISCUSSION

#### A. Stress dependence of the resistance

The measured resistance of  $n$ -type GaAs changes under stress because of changes in carrier effective mass, scattering times, sample dimensions, and possible carrier redistribution effects. For GaAs for  $\chi$  less than 5 kbar, the latter contribution is negligible unless partially ionized deep traps are present. This case is discussed in Sec. III D.

All relative contributions can be estimated from the equation describing scattering lifetimes for polar-optic scattering,<sup>46</sup> since polar-optic scattering dominates other scattering mechanisms in GaAs at room temperature.<sup>18,46,59,60</sup> We have for  $n$ -type material

$$R = \rho l/A = l m_c^*/n e^2 \tau A, \quad (1)$$

where  $\rho$  is the resistivity,  $l$  and  $A$  are the sample length and cross-section-area dimensions,  $m_c^*$  is the effective mass of the conduction band,  $n$  is the electron concentration in the  $\Gamma_1^C$  conduction-band minimum, and  $\tau$  is the scattering lifetime. The quantities  $m_c^*$  and  $\tau$  are the scalar projections of the corresponding tensors evaluated in the direction of current flow. For polar-optical scattering<sup>46</sup> in an isotropic model

$$\tau = \frac{\Omega_V M (\hbar \omega_0)^{5/2}}{4\pi (2m_c^*)^{1/2} e^2 e^* k T} \frac{e^\theta - 1}{\theta}, \quad (2a)$$

where

$$\theta = \hbar \omega_0 / k T, \quad (2b)$$

and where  $\Omega_V$  is the volume of the unit cell,  $M$  is the reduced atomic mass,  $\omega_0$  is the longitudinal-optical-phonon frequency near  $k=0$ , and  $e^*$  is the effective ionic charge.

Obviously, the dependence of  $R$  on stress, as given by the many stress-dependent parameters in Eqs. (1) and (2), is not straightforward. However, previous hydrostatic data<sup>26,58</sup> indicated agreement with a simple  $R \propto m_c^{*3/2}$  power-law dependence. The total relative hydrostatic stress dependence of the resistance may be evaluated from Eqs. (1) and (2) to yield

$$\frac{\Delta R}{R} = \frac{\Delta l}{l} + \frac{3}{2} \frac{\Delta m_c^*}{m_c^*} + 2 \frac{\Delta e^*}{e^*} - \frac{\Delta A}{A} - \frac{5}{2} \frac{\Delta \omega_0}{\omega_0} + \left(1 - \frac{\theta e^\theta}{e^\theta - 1}\right) \frac{\Delta \theta}{\theta}. \quad (3)$$

Because the hydrostatic pressure dependences of  $\omega_0$ ,<sup>61</sup>  $e^*$ ,<sup>61</sup> and  $m_c^*$ ,<sup>62</sup> have been measured directly and the coefficients of the compliance tensor are known,<sup>63</sup> Eqs. (1) and (2) may be evaluated for hydrostatic stress. All relevant values are summarized in Table I, evaluated for convenience for an assumed hydrostatic stress of  $\frac{10}{3}$  kbar, which corresponds to a uniaxial stress to 10 kbar. Calculated dimensional changes for 10-kbar [100] and [111] uniaxial stresses are also given.

When all contributions expressed by Eq. (3) are added, the predicted value  $\Delta R/R_{\text{calc}} = 0.0150$  is less than half the experimental value  $\Delta R/R = 0.0340$ . If only the mass term is considered and all others neglected, then  $\Delta R/R$  is calculated to be 0.0350, and excellent agreement is obtained. This is the origin of the previous apparent agreement between theory and experiment for hydrostatic stress. The above analysis shows, however, that this agreement is only superficial and cannot be justified on a microscopic basis. For the purpose of further analysis of particularly the low-stress results, we shall continue to assume that the stress-induced resistance change is dominated by the stress-induced changes in sample dimensions and in the mass tensor, although we emphasize that this is only a hypothesis to assist the understanding of the results. Indeed, free-carrier absorption results on GaAs by Walton and Metcalfe appear to be interpretable only in terms of a stress-induced anisotropy in the scattering time which is comparable to that induced in the effective mass.<sup>64</sup>

#### B. Low-stress (linear-piezoresistance) results

The theory of stress dependence of  $m_c^*$  for hydrostatic and uniaxial stresses for all two-band and three-band terms in the Pikus-Bir Hamiltonian<sup>65</sup> was given in a four-band model in a previous paper.<sup>47</sup> Explicit expressions were obtained in terms of the pseudopotential parameters and other data summarized in Table II. Here,  $a_0$  is the lattice constant,<sup>66</sup>  $v_3^s, \dots, v_{12}^s$  are pseudopotential form factors,<sup>35</sup> the derivatives  $v_j^s$  and  $\bar{v}_j^s$  are defined in terms of the  $v_j^s$  as<sup>67</sup>

$$v_j^s = G \frac{dv_j^s}{dG}, \quad (4a)$$

$$\bar{v}_j^s = V \frac{dv_j^s}{dV} = -\left(\frac{1}{3}v_j^s + v_j^s\right); \quad (4b)$$

$\zeta$  represents the phonon terms,<sup>67</sup>  $S_{11}$ ,  $S_{12}$ , and  $S_{44}$  are the compliance coefficients,<sup>63</sup>  $\Omega = (2\pi\hbar)^2 / 2m_0a_0^2$ , the  $\beta$  and  $\gamma$  parameters are mixing coefficients given in Ref. 47, and the strains  $\epsilon_H$ ,  $\epsilon_T$ , and  $\epsilon_R$  are given for a uniaxial stress  $\chi_T$  or  $\chi_R$  parallel to [100] or [111], respectively, by

$$\epsilon_H = \frac{1}{3}(S_{11} + 2S_{12})\chi_{T,R}, \quad (5a)$$

$$\epsilon_T = \frac{2}{3}(S_{11} - S_{12})\chi_T, \quad (5b)$$

$$\epsilon_R = \frac{1}{6}S_{44}\chi_R. \quad (5c)$$

The energies  $E_0$  and  $\Delta_0$  are the fundamental absorption threshold<sup>68</sup> and spin-orbit splitting of the upper valence band, while  $\bar{E}_0'$  and  $\bar{E}_0''$  represent the average energy between the upper-valence and second<sup>37</sup> and third,<sup>69</sup> respectively, conduction bands at  $\Gamma$  calculated with the spin-orbit splittings removed.

The data of Table II lead to the matrix elements and self-energies summarized in Table III. These values are compared to experiment<sup>48,70</sup> where possible. As with Ge,<sup>47</sup> the results agree within 20% establishing the level of confidence of the model calculation.

Table IV summarizes the calculated values of  $m_c^*$  in directions parallel and perpendicular to the applied stress, although only the parallel component is used here. The bilinear, two-band con-

TABLE II. Values of pseudopotential and other parameters for GaAs, used to evaluate matrix elements and stress-induced changes in the effective mass.

Data	Calculated values
$a_0/a_B = 10.684^a$	$\Omega = 4.71 \text{ eV}$
$v_3^s = -3.27 \text{ eV}^b$	$\beta'_{25} = 0.831$
$v_4^s = -1.77 \text{ eV}^c$	$\gamma'_{25} = 0.556$
$v_8^s = 0.44 \text{ eV}^b$	$\beta'_2 = 0.848$
$v_{11}^s = 1.12 \text{ eV}^b$	$\gamma'_2 = 0.530$
$v_{12}^s = 0.82 \text{ eV}^c$	$\bar{v}'_3 = 1.09 \text{ eV}$
$v'_3 = 6.53 \text{ eV}^c$	$\bar{v}'_8 = -1.94 \text{ eV}$
$v'_4 = 6.33 \text{ eV}^c$	$\bar{v}'_{11} = -1.57 \text{ eV}$
$v'_8 = 4.49 \text{ eV}^c$	$\epsilon_H = -0.00139$
$v'_{11} = 1.36 \text{ eV}^c$	$\epsilon_T = -0.01125$
$v'_{12} = 0.16 \text{ eV}^c$	$\epsilon_R = -0.0031$
$\zeta = 0.66^c$	
$S_{11} = 12.64 \times 10^{-4} \text{ kbar}^{-1d}$	
$S_{12} = -4.234 \times 10^{-4} \text{ kbar}^{-1d}$	
$S_{44} = 18.6 \times 10^{-4} \text{ kbar}^{-1d}$	
$E_0 = 1.423 \text{ eV (300 K)}^e$	
$\Delta_0 = 0.341 \text{ eV}^f$	
$\bar{E}'_0 = 4.69 \text{ eV}^f$	
$\bar{E}''_0 = 10.53 \text{ eV}^g$	

<sup>a</sup>Wyckoff, Ref. 66.

<sup>b</sup>Pandey and Phillips, Ref. 35.

<sup>c</sup>Cardona, Ref. 67; Ge values.

<sup>d</sup>Huntington, Ref. 63.

<sup>e</sup>Sell, Ref. 68.

<sup>f</sup>Aspnes and Studna, Ref. 37.

<sup>g</sup>Aspnes, Olson, and Lynch, Ref. 69.

TABLE III. Values of matrix elements and self-energy terms for GaAs, calculated from the pseudo-potential model of Ref. 47 and from data summarized in Table II.

Quantity	Calc. value	Expt. value
$P$	$1.05 \hbar G_0$	
$Q$	$0.83 \hbar G_0$	
$R$	$0.45 \hbar G_0$	
$c_T$	17.26 eV	
$c_{R1}$	-32.64 eV	
$c_{R2}$	1.26 eV	
$a_{25'}$	-5.57 eV	
$a_{2'}$	-17.72 eV	
$a_{15}$	-7.48 eV	
$a_{12'}$	-8.68 eV	
$a$	-12.15 eV	$-8.3 \pm 0.8 \text{ eV}^a$ ; $-10.0 \pm 0.1^b$
$b_{25'}$	-7.26 eV	
$b_{15}$	4.49 eV	
$b_{12'}$	-14.35 eV	
$b$	-2.42 eV	$-1.7 \pm 0.1 \text{ eV}^a$
$d_{25'}$	-20.26 eV	
$d_{15}$	-17.96 eV	
$d$	-5.85 eV	$-4.55 \pm 0.25^a$

<sup>a</sup>Chandrasekhar and Pollak, Ref. 70.

<sup>b</sup>Welber *et al.*, Ref. 48.

tributions are shown explicitly. The results, expressed in terms of a relative resistance change,  $\Delta R/R$ , assuming a  $\frac{3}{2}$  power-law dependence on the mass and including dimensional changes as discussed in Sec. IIIA, are summarized in Table V.

The favorable comparison between theory and experiment seen in Table V shows that the observed behavior of  $\Delta R/R$  is well represented by changes in the effective mass tensor of the  $\Gamma_1^C$  conduction-band minimum. In particular, the complete theory gives a good accounting of the anisotropy of this change. The previous two-band model, which included only the contribution from the change in energy denominator, predicts negligible anisotropy as seen in the two-band column in Table IV. If one assumed that  $\Delta R/R \sim m_c^*$  instead of  $(m_c^*)^{3/2}$ , the agreement would be better. Such behavior in fact could be argued on theoretic

cal grounds for the pure shear contributions by noting that the average values of  $m_c^*$ ,  $\omega_0$ , and  $e^*$  are independent of shear stress to first order for the nondegenerate  $\Gamma_1^C$  minimum, and thus if the scattering were isotropic in the unstressed case it should also be independent of shear to first order in the stressed case. This would change the  $(m_c^*)^{-3/2}$  dependence to  $(m_c^*)^{-1}$ . However, this point is minor considering the existing uncertainties in the scattering model.

Surprisingly, previous uniaxial stress piezoresistance work<sup>19,24,42,43</sup> on GaAs has failed to show any anisotropy in the linear-stress region (the effect is masked by intervalley carrier redistribution effects in Ge, Si, and other semiconductors). This may be due to appreciable hydrostatic stress components generated in the previously used stress configurations. This is expected in geometries where the uniaxial stress is applied along the short dimension; in fact, the same approach on an exaggerated scale is used by Pitt and Lees<sup>25,26</sup> to achieve hydrostatic stress. This emphasizes the experimental difficulties in attaining pure uniaxial stress.

### C. High-stress (superlinear-piezoresistance) results

For uniaxial stress greater than 5 kbar, carrier transfer occurs via thermal activation to low-mobility indirect minima and the resistance shows a superlinear increase with increasing  $\chi$ . With two types of minima, we have for  $j=x$  or  $L$ ,

$$R(\chi)/R(0) = \{[n_\Gamma(\chi)\mu_\Gamma(\chi) + n_j(\chi)\mu_j(\chi)]eR(0)\}^{-1} \quad (6a)$$

$$\cong [n_\Gamma(0)\mu_\Gamma(0)]/[n_\Gamma(\chi)\mu_\Gamma(\chi)]. \quad (6b)$$

Because<sup>16</sup>  $\mu_\Gamma \cong 7350 \text{ cm}^2\text{V}^{-1}\text{sec}^{-1}$  is much greater than  $\mu_L \cong 920 \text{ cm}^2\text{V}^{-1}\text{sec}^{-1}$  and  $\mu_X \cong 300 \text{ cm}^2\text{V}^{-1}\text{sec}^{-1}$ , the conductance in the higher minima can be neglected and Eq. (6b) follows from Eq. (6a). Solving the charge neutrality equation in the Boltzmann approximation for a constant carrier concentration leads to the result

$$R(\chi)/R(0) \cong \mu_\Gamma(\chi)/\mu_\Gamma(0) + \delta R(\chi)/R(0), \quad (7a)$$

$$\delta R(\chi)/R(0) = (N_j/N_\Gamma) \exp[-E_{j\Gamma}(\chi)/kT], \quad (7b)$$

TABLE IV. Calculated first-order stress-induced changes in the reciprocal conduction-band mass  $m_e/m_c^* = 14.66$  ( $m_c^* = 0.0682 m_e$ ) for GaAs, at 300 K at 10-kbar uniaxial stress (3.33-kbar hydrostatic pressure).

Component	Bilinear	Two-band	Three-band	Shear only	Total, shear and hydrostatic	
Hydrostatic	0.038	-0.459	0	0	-0.421	
Tetragonal shear	$\parallel$	0.307	0.730	-0.505	0.532	0.111
	$\perp$	-0.154	-0.365	0.253	-0.266	-0.687
Trigonal shear	$\parallel$	0.169	0.494	-0.800	-0.137	-0.558
	$\perp$	-0.085	-0.247	0.400	0.068	-0.353

TABLE V. Calculated and experimental values of first-order changes in resistance, including only mass and dimensionality change contributions, for 10-kbar uniaxial stress (3.33-kbar hydrostatic pressure).

	Hydrostatic	[100] uniaxial	[111] uniaxial
$\frac{\Delta l}{l} - \frac{\Delta A}{A}$	+0.0014	-0.021	-0.011
$\frac{3}{2} \left( \frac{\Delta m_c^*}{m_c^*} \right)_{\parallel}$	+0.043	-0.011	0.057
$\left( \frac{\Delta R}{R'} \right)_{\text{calc}}$	0.045	-0.032	0.046
$\left( \frac{\Delta R}{R'} \right)_{\text{expt}}$	$0.034 \pm 0.005$	$0.000 \pm 0.005$	$0.040 \pm 0.005$

where  $\delta R(\chi)$  is the superlinear component and  $E_{j\Gamma} = E_j - E_{\Gamma}$ .

In practice, the deformation potentials are such that only the single indirect minimum in the uniaxial stress direction ( $X_1^{C[100]}$  for [100] stress and  $L_1^{C[111]}$  for [111] stress) can contribute to the superlinear term. Thus we consider only those two cases, where  $N_j = N_X^{[100]}$  or  $N_L^{[111]}$  is the density of states of a single indirect minimum. We then have in general

$$\ln \left( \frac{\delta R(\chi)}{R(0)} \right) = \ln \left( \frac{N_j^u}{N_{\Gamma}} \right) - \frac{E_{j\Gamma}(0) + \chi dE_{j\Gamma}^u/d\chi}{kT}, \quad (8)$$

where for [100] stress

$$\frac{dE_{X\Gamma}^{[100]}}{d\chi} = \left( \frac{dE_{X\Gamma}}{d\chi} \right)_H + \frac{\epsilon_T \mathcal{E}_2^X}{\chi}, \quad (9a)$$

and for [111] stress

$$\frac{dE_{L\Gamma}^{[111]}}{d\chi} = \left( \frac{dE_{L\Gamma}}{d\chi} \right)_H + \frac{2\epsilon_R \mathcal{E}_2^L}{\chi}, \quad (9b)$$

where the  $(dE/d\chi)_H$  terms represent the corresponding equivalent hydrostatic stress dependences, the  $\mathcal{E}_2$  terms represent the corresponding shear deformation potentials, and the strains are defined in Eqs. (5). Because the hydrostatic stress dependences of  $\Gamma_1^C$ ,  $L_1^C$ , and  $X_1^C$  relative to the  $\Gamma_8^V$  valence-band maximum, and the  $\Gamma$ ,  $L$ , and  $X$  state densities, are known,<sup>16,48,71</sup> it is possible in principle to determine the zero-stress indirect threshold and the indirect-threshold shear deformation potentials from a logarithmic plot of  $\delta R(\chi)/R(0)$  vs  $\chi$ .

For degenerate material, the above expressions have to be modified slightly. Here, the reference energy becomes  $E_F(\chi)$  instead of  $E_{\Gamma}(\chi)$ , and the density of states  $N_{\Gamma}$  must be replaced by the zero-stress degenerate carrier concentration  $n_{\Gamma}(0) = N_D^*$ , where  $N_D^*$  is the concentration of ionized

donors. For GaAs with  $N_D^* = 3.8 \times 10^{18} \text{ cm}^{-3}$ , the Fermi level lies 87 meV above the  $\Gamma_1^C$  conduction-band minimum.<sup>72</sup>

Figure 4 shows the results of semilogarithmic plots of the relative superlinear component for representative [111] stress results from three sources: our  $7 \times 10^{16} \text{ cm}^{-3}$  material, our  $3.8 \times 10^{18} \text{ cm}^{-3}$  material, and data taken from Pickering and Adams<sup>43</sup> on bulk material for which  $n_{\Gamma}(0) \cong 2 \times 10^{15} \text{ cm}^{-3}$ . Good straight-line plots are obtained. The slopes of these plots show that the  $L_1^C - \Gamma_1^C$  separation decreases at 14.4 and 19.2 meV/kbar for the moderately and degenerately doped samples, respectively. The former is in good agreement with the value  $14.5 \pm 1.5 \text{ meV/kbar}$  obtained by Pickering and Adams.<sup>43</sup> Using the  $\Gamma_1^C$  and  $L_1^C$  hydrostatic shifts of 12.6 meV/kbar,<sup>48</sup> and 5.5 meV/kbar,<sup>16,71</sup> relative to  $\Gamma_8^V$  we find  $\mathcal{E}_2^L = 19.6 \pm 3 \text{ eV}$ , in very good agreement with previously measured values of  $16.2 \pm 0.4 \text{ eV}$  for Ge,<sup>49</sup>

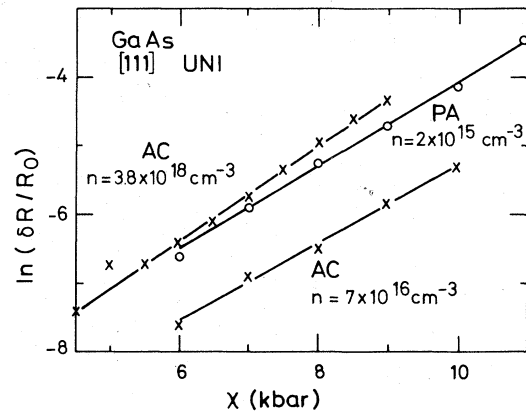


FIG. 4. Variation of the superlinear piezoresistance component measured here for [111] stress for moderately and heavily doped samples (AC, this work). Data from Pickering and Adams (PA, Ref. 43) are also shown.

and  $16.0 \pm 3.5$  eV for GaSb.<sup>50</sup>

Pickering and Adams<sup>43</sup> obtained a somewhat larger deformation potential  $\mathcal{E}_2^L = 22 \pm 3$  eV, because they used the older values<sup>71</sup> 11 and 5.0 meV/kbar for the  $\Gamma_1^C$  and  $L_1^C$  hydrostatic shifts relative to  $\Gamma_8^V$ . This shows that the calculated values of  $\mathcal{E}_2$  are relatively sensitively dependent upon outside variables. A calculation of  $\mathcal{E}_2^L$  for the data from the degenerately doped material leads to the anomalously large value of 27 eV, possibly due to its generally poorer crystal quality as also evidenced by its inability to withstand more than 4 kbar of [100] stress.

From the  $\mathcal{E}_2^L$  data, the density of states ratio  $N_L^{[111]}/N_T = 6.5$ ,<sup>16</sup> and Eqs. (8) and (9), we find  $E_{LR}(0)$  values of 330 meV for the moderately doped material and 360 meV for the degenerately doped material. The latter value is reduced to 320 meV if  $\mathcal{E}_2^L = 14.5$  meV/kbar is used rather than the higher value measured with these samples. Thus all values are consistent with a separation  $E_{LR}(0) = 330 \pm 40$  meV, to be compared with the value  $300 \pm 30$  meV obtained by Pickering and Adams.<sup>43</sup>

All the [111] piezoresistance data provide an independent measure of the zero-stress  $L_1^C - \Gamma_1^C$  energy separation, which complements the previous value of  $285 \pm 30$  meV at 300 K deduced<sup>16</sup> from core-level electroreflectance measurements.<sup>40</sup> Because the latter separation value was obtained by assuming a constant electron-hole interaction energy for core-level transitions for both  $L_1^C$  and  $X_1^C$ , this result provides an independent verification of the validity of this assumption to within experimental error. It should be noted, however, that the binding energies for the Ga-3d core-lower-conduction-band excitons in the Ga-V compounds fall in the 100–200-meV range,<sup>73,74</sup> and the variation of the exciton Rydberg over the lower conduction band could be as much as 30% of this value and still be consistent with experimental uncertainties. Because the stress values are less well defined, they should be viewed as supporting the more accurate comprehensive model.<sup>16</sup>

For [100] stress the picture is much less clear. Because of the previous conviction that the  $\langle 100 \rangle$  minima were the first indirect minima, more [100] stress data are available that apparently show activation into  $\langle 100 \rangle$  minima but some of these data<sup>19,24</sup> were taken with the questionable “pancake” geometry and should not be considered reliable. The Pickering and Adams data, and those reported here, show much less consistency than do the [111] stress results. Unfortunately, our degenerately doped samples could not be stressed sufficiently before fracture to reach the superlinear region for [100] stress.

Existing apparent carrier transfer data from

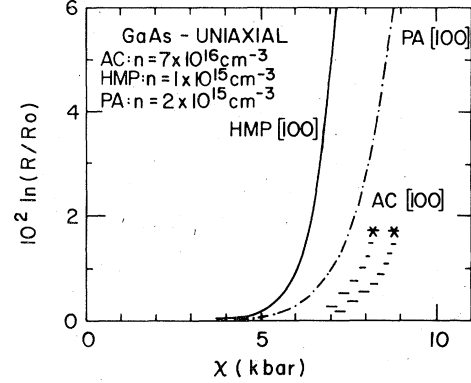


FIG. 5. As with Fig. 1, but with two sets of data from this paper (AC, this work), and previous results from Harris, Moll, and Pearson (HMP, Ref. 24) and Pickering and Adams (PA, Ref. 43).

four sources are shown in Fig. 5. It should be noted that our bar samples fractured soon after the onset of superlinear resistance. However, the cubic (Ref. 43) and “pancake” (Ref. 24) samples were able to withstand much higher stress, suggesting again that the stress here was probably not purely uniaxial. If one performs a carrier-transfer analysis of these data similar to that performed for [111] stress, using the hydrostatic stress shift of  $-1.5$  meV/kbar (Ref. 71) for the  $X_1^C$  minima relative to  $\Gamma_8^V$  and the uniaxial stress shifts of 28 and 36 meV/kbar for our moderately doped samples, one finds that  $\mathcal{E}_2^L$  should lie in the 25–30-eV range. The value obtained by Pickering and Adams is somewhat smaller, of the order of 20 eV. These values are substantially greater than those observed for similar materials,  $8.6 \pm 0.2$  eV for Si,<sup>49</sup>  $5.4 \pm 0.3$  eV for AlSb,<sup>51</sup> and  $6.9 \pm 0.7$  eV for GaP.<sup>52</sup> It is also possible to estimate  $\mathcal{E}_2^X$  from pseudopotential theory in a simple two-band  $X_1^C, X_1^V$  model, using the stress-dependent pseudopotentials of the previous paper<sup>47</sup> and the pseudopotential wave functions of Ref. 67. The result can be expressed in terms of the parameters summarized in Table II as

$$\Delta E_X^{[100]} = \epsilon_T \mathcal{E}_2^X / \chi = \epsilon_T [2\Omega(\beta_x^2 - \gamma_x^2) + \frac{1}{2}v_8^2\beta_x^2], \quad (10)$$

where

$$\gamma_x/\beta_x = 2\sqrt{2}v_3^s / \{\Omega + v_8^s + [(\Omega + v_8^s)^2 + 8v_3^{s2}]^{1/2}\}, \quad (11a)$$

$$\beta_x^2 + \gamma_x^2 = 1. \quad (11b)$$

We find  $\mathcal{E}_2^X \cong 6.3$  eV, in good agreement with the non-GaAs data but again contradicting the GaAs results.

Further inconsistencies result if we estimate  $E_{XT}(0)$  from these data. This energy separation ranges from a low of 310 meV from the Pickering-



Adams result<sup>43</sup> to highs of 420 and 470 meV using the results of the present paper.

Primarily because of the anomalously high  $\mathcal{G}_2^X$  values, we must consider alternative explanations to these apparent carrier activation results. There exist at least two possibilities: anomalous behavior of the strain as stresses approach the fracture limit, with possible irreversible increases in resistance because of stress-induced defects, or else transfer of carriers to deep traps associated with the  $X_1^C$  minima. Unfortunately, the first explanation could not be verified with our samples, which broke soon after the appearance of the superlinear component. The second explanation is possible because deep traps associated with  $X_1^C$  have been observed in transport<sup>26</sup> measurements under large hydrostatic pressure, although these traps are quite sample dependent and, if they appear for  $X_1^C$  minima, should also be expected to appear for the  $L_1^C$  minima.

By contrast to the case for [111] stress, the [100] stress behavior has not been satisfactorily resolved and further work is needed.

#### D. Lightly doped samples

The data in Fig. 1 were obtained from a sample dominated by a deep trap of density of  $6.5 \times 10^{16}$  cm<sup>-3</sup>, located 210 meV below the bottom of the conduction band. The expected stress variation can be calculated by considering only the trap and the  $\Gamma_1^C$  minimum. We have

$$N_D^* = N_D \{1 + \exp[-(E_D - E_F)/KT]\}^{-1}, \quad (12a)$$

$$n_\Gamma = N_\Gamma \exp[-(E_C - E_F)/KT], \quad (12b)$$

where  $E_D$  is the trap energy,  $E_F$  is the Fermi level, and  $N_\Gamma = 4 \times 10^{17}$  cm<sup>-3</sup> is the density of states of the  $\Gamma_1^C$  minimum at 300 K. Charge neutrality leads to the approximate solution

$$n_\Gamma \cong (N_\Gamma N_D)^{1/2} \exp[-(E_C - E_D)/2KT], \quad (13)$$

which is valid for the conditions of this experiment. Therefore, we have

$$\ln\left(\frac{R(\chi)}{R(0)}\right) \cong \frac{\mu(0)}{\mu(\chi)} + \frac{\chi}{2kT} \frac{dE_{CD}}{d\chi}. \quad (14)$$

Straight-line behavior is observed, as predicted. In principle, the mobility ratio can be obtained from Sec. III B; it should not contribute for [100] stress and at most will make a 6% correction to the hydrostatic pressure and [111] stress data.

Including the mobility correction, we find that  $E_D$  moves relative to the  $\Gamma_8^V$  valence-band edge as 1.0, 0.7, and 0.2 meV/kbar for hydrostatic, [100],

and [111] uniaxial stresses, respectively. For comparison, the  $\Gamma_1^C$ ,  $L_1^C$ , and  $X_1^C$  minima vary as 4.2, 1.8, and -0.5 meV/kbar, respectively. Thus the deep trap can be considered as a mixture of  $L_1^C$  and  $X_1^C$  states, with a small contribution from  $\Gamma_1^C$ , which is what one anticipates from the theory of deep traps,<sup>75,76</sup> the proximity of the trap to the conduction band, and the relative densities of states of the three types of conduction-band minima.

The different rates of variation with stress for the different types of stress are outside the experimental uncertainty. They cannot be interpreted in terms of the changing consistency of the trap wave function in the standard effective-mass parametrization, however, because the shear terms cancel out. This can be seen easily as follows. In any effective-mass model, the minima are described in terms of effective-mass tensors and conduction-band edge energies, and the trap energy is obtained by solving an eigenvalue equation of the general form

$$0 = \sum_\nu f_\nu (E_D - E_\nu), \quad (14)$$

where the index  $\nu$  runs over the  $\Gamma$  minimum and each of the four  $L$  and three  $X$  minima. We suppose that a stress is applied. Then Eq. (14) may be solved for  $dE_D/d\chi$ . If a  $k$ -star degeneracy is lifted by the shear term in a uniaxial stress, this has no effect to first order since the shear induces no net shift of the center of gravity of the minima. Thus only the hydrostatic terms survive, and consequently a simple effective-mass approach predicts no difference in behavior between stresses. This is not in accordance with experiment.

*Note added in proof.* Recent four-contact piezoresistance measurements by C. N. Ahmad and A. R. Adams on high-purity vapor-epitaxy samples with a 2:1 length-width ratio show no superlinear piezoresistance for [100] uniaxial stresses up to 10 kbar [A. R. Adams (private communication); see also note added in proof in Ref. 43]. This result confirms our conclusion based on the anomalously large deformation potential that some mechanism other than transfer to an  $X_1^C$  minimum must be responsible for the superlinear piezoresistance of GaAs for [100] stress.

#### ACKNOWLEDGMENTS

One of us (D.E.A.) wishes to thank the Alexander von Humboldt Foundation and the Max-Planck-Institut für Festkörperforschung for their kind

support and hospitality during the course of this work. Thanks are also due in particular to M. Paesler and G. Fischer for performing the Hall and resistivity measurements to characterize the

materials, and to C. Pickering and A. R. Adams for a preliminary report of their work prior to publication.

- \*Work at the Max-Planck-Institut für Festkörperforschung supported in part by the Alexander von Humboldt Foundation.
- †Permanent address.
- <sup>1</sup>R. Barrie, F. A. Cunnell, J. T. Edmond, and I. M. Ross, *Physica (Utr.)* **20**, 1087 (1954).
  - <sup>2</sup>A. Sagar, *Phys. Rev.* **112**, 1533 (1958).
  - <sup>3</sup>L. C. Barcus, A. Perlmutter, and J. Callaway, *Phys. Rev.* **111**, 167 (1958); **115**, 1778(E) (1959).
  - <sup>4</sup>M. Glicksman, *J. Phys. Chem. Solids* **8**, 511 (1959).
  - <sup>5</sup>W. G. Spitzer and J. M. Whelan, *Phys. Rev.* **114**, 59 (1959).
  - <sup>6</sup>T. S. Moss and A. K. Walton, *Proc. Phys. Soc. Lond.* **74**, 131 (1959).
  - <sup>7</sup>O. G. Folberth (unpublished). The data were cited by Welker and Weiss (Ref. 8).
  - <sup>8</sup>H. Welker and H. Weiss, *Solid State Physics*, Vol. 3, edited by F. Seitz and D. Turnbull (Academic, New York, 1956), p. 1.
  - <sup>9</sup>O. G. Folberth and H. Weiss, *Z. Naturforsch. A* **10**, 615 (1955).
  - <sup>10</sup>J. T. Edmond, R. F. Broom, and F. A. Cunnell, *Rugby Semiconductor Conference* (The Physical Society, London, 1956).
  - <sup>11</sup>P. V. Gray and H. Ehrenreich, *Bull. Am. Phys. Soc.* **3**, 255 (1958).
  - <sup>12</sup>J. Callaway, *J. Electronics* **2**, 330 (1957).
  - <sup>13</sup>A. L. Edwards, T. E. Slykhouse, and H. G. Drickamer, *J. Phys. Chem. Solids* **11**, 140 (1958).
  - <sup>14</sup>T. E. Slykhouse and H. G. Drickamer, *J. Phys. Chem. Solids* **7**, 210 (1958).
  - <sup>15</sup>W. Paul and D. M. Warschauer, *J. Phys. Chem. Solids* **5**, 102 (1958).
  - <sup>16</sup>D. E. Aspnes, *Phys. Rev. B* **14**, 5331 (1976).
  - <sup>17</sup>H. Ehrenreich and D. J. Olechna, *Bull. Am. Phys. Soc.* **5**, 151 (1960).
  - <sup>18</sup>H. Ehrenreich, *Phys. Rev.* **120**, 1951 (1960).
  - <sup>19</sup>M. Shyam, J. W. Allen, and G. L. Pearson, *IEEE Trans. Electron Dev.* **ED-13**, 63 (1966).
  - <sup>20</sup>A. R. Hutson, A. Jayaraman, and A. S. Coriell, *Phys. Rev.* **155**, 786 (1967).
  - <sup>21</sup>L. W. James, R. C. Eden, J. L. Moll, and W. E. Spicer, *Phys. Rev.* **174**, 909 (1968).
  - <sup>22</sup>I. Balslev, *Phys. Rev.* **173**, 762 (1968).
  - <sup>23</sup>L. W. James and J. L. Moll, *Phys. Rev.* **183**, 740 (1969).
  - <sup>24</sup>J. S. Harris, J. L. Moll, and G. L. Pearson, *Phys. Rev. B* **1**, 1660 (1970).
  - <sup>25</sup>G. D. Pitt and J. Lees, *Solid State Commun.* **8**, 491 (1970).
  - <sup>26</sup>G. D. Pitt and J. Lees, *Phys. Rev. B* **2**, 4144 (1970).
  - <sup>27</sup>M. G. Craford, R. W. Shaw, A. H. Herzog, and W. O. Groves, *J. Appl. Phys.* **43**, 4075 (1972).
  - <sup>28</sup>A. Onton, R. J. Chicotka, and Y. Yacoby, in *Proceedings of the Eleventh International Conference on the Physics of Semiconductors, Warsaw* (Polish Scientific, Warszawa, 1972), p. 1023.
  - <sup>29</sup>P. Blood, *Phys. Rev. B* **6**, 2257 (1972).
  - <sup>30</sup>M. Cohen and T. K. Bergstresser, *Phys. Rev.* **141**, 789 (1966).
  - <sup>31</sup>J. Van Vechten, *Phys. Rev.* **187**, 1007 (1969).
  - <sup>32</sup>F. H. Pollak, C. W. Higginbotham, and M. Cardona, *J. Phys. Soc. Jpn. Suppl.* **21**, 20 (1966).
  - <sup>33</sup>F. Herman, R. L. Kortum, C. D. Kuglin, and J. P. Van Dyke, in *Methods of Computational Physics*, edited by B. Alder, S. Fernbach, and M. Rotenberg (Academic, New York, 1968), p. 193.
  - <sup>34</sup>D. J. Stukel, T. C. Collins, and R. N. Euwema, in *Electronic Density of States*, edited by L. H. Bennett, Natl. Bur. Stds. Spec. Publ. No. 323 (U.S. GPO, Washington, D.C., 1971), p. 93.
  - <sup>35</sup>K. C. Pandey and J. C. Phillips, *Phys. Rev. B* **9**, 1552 (1974).
  - <sup>36</sup>J. R. Chelikowsky and M. L. Cohen, *Phys. Rev. Lett.* **32**, 674 (1974); *Phys. Rev. B* **14**, 556 (1976).
  - <sup>37</sup>D. E. Aspnes and A. A. Studna, *Phys. Rev. B* **7**, 4605 (1973).
  - <sup>38</sup>W. D. Grobman and D. E. Eastman, *Phys. Rev. Lett.* **29**, 1508 (1972).
  - <sup>39</sup>R. Pollak, L. Ley, S. Kowalczyk, D. A. Shirley, J. D. Joannopoulos, D. J. Chadi, and M. L. Cohen, *Phys. Rev. Lett.* **29**, 1103 (1973).
  - <sup>40</sup>D. E. Aspnes, C. G. Olson, and D. W. Lynch, *Phys. Rev. Lett.* **37**, 766 (1976).
  - <sup>41</sup>D. E. Aspnes, *Inst. Phys. Conf. Ser. No. 33b*, 110 (1977).
  - <sup>42</sup>P. J. Vinson, C. Pickering, A. R. Adams, W. Fawcett, and G. D. Pitt, in *Proceedings of the Thirteenth International Conference on the Physics of Semiconductors, Rome*, edited by F. G. Fumi (Tipografia Marves, Rome, 1976), p. 1243.
  - <sup>43</sup>C. Pickering and A. R. Adams, *J. Phys. C* **10**, 3115 (1977).
  - <sup>44</sup>R. Dingle, R. A. Logan, and J. R. Arthur, Jr., in *Gallium Arsenide and Related Compounds* (Edinburgh), 1976, edited by C. Hilsum, *Inst. Phys. Conf. Ser. No. 33a*, 210 (1977).
  - <sup>45</sup>R. Trommer and M. Cardona, *Solid State Commun.* **21**, 153 (1977).
  - <sup>46</sup>H. Ehrenreich, *J. Appl. Phys. (Suppl.)* **32**, 2155 (1961).
  - <sup>47</sup>D. E. Aspnes and M. Cardona, preceding paper, *Phys. Rev. B* **17**, 726 (1978).
  - <sup>48</sup>B. Welber, M. Cardona, C. K. Kim, and S. Rodriguez, *Phys. Rev. B* **12**, 5729 (1975).
  - <sup>49</sup>I. Balslev, *Phys. Rev.* **143**, 636 (1966).
  - <sup>50</sup>A. K. Walton and S. F. Metcalfe, *J. Phys. C* **9**, 3855 (1976).
  - <sup>51</sup>L. D. Laude, M. Cardona, and F. H. Pollak, *Phys. Rev. B* **1**, 1436 (1970).
  - <sup>52</sup>I. Balslev, *J. Phys. Soc. Jpn. Suppl.* **21**, 101 (1966). Balslev's quoted value for  $\mathcal{E}_2^x$  was determined from estimated values of the compliance coefficients  $S_{11}$  and  $S_{12}$ . The value that we use is Balslev's value re-

- vised to account for more recent, measured values of the compliance coefficients [see R. Weil and W. O. Groves, *J. Appl. Phys.* **39**, 4049 (1968)].
- <sup>53</sup>D. V. Lang (private communication).
- <sup>54</sup>H. Fritsche, *Phys. Rev.* **115**, 336 (1959).
- <sup>55</sup>F. H. Pollak, *Phys. Rev.* **133**, A618 (1965).
- <sup>56</sup>F. H. Pollak and M. Cardona, *Phys. Rev.* **172**, 816 (1968).
- <sup>57</sup>Manufactured by High Pressure Equipment Co., Inc., Erie, Pa. 16505.
- <sup>58</sup>A. Sagar, *Phys. Rev.* **112**, 1533 (1958).
- <sup>59</sup>D. L. Rode, *Phys. Rev. B* **2**, 1012 (1970).
- <sup>60</sup>D. L. Rode and S. Knight, *Phys. Rev. B* **3**, 2534 (1971).
- <sup>61</sup>R. Trommer, E. Anastassakis, and M. Cardona, in *Light Scattering in Solids*, edited by M. Balkanski, R. C. C. Leite, and S. P. S. Porto (Flammarion, Paris, 1976), p. 396.
- <sup>62</sup>G. D. Pitt, J. Lees, R. A. Hoult, and R. A. Stradling, *J. Phys. C* **6**, 3282 (1973).
- <sup>63</sup>H. B. Huntington, in Ref. 8, 1968, p. 213.
- <sup>64</sup>A. K. Walton and S. F. Metcalf, *J. Phys. C* **9**, 3605 (1976).
- <sup>65</sup>G. E. Pikus and G. L. Bir, *Fiz. Tverd. Tela* **1**, 1642 (1959) [*Sov. Phys.-Solid State* **1**, 1502 (1959)].
- <sup>66</sup>R. W. G. Wyckoff, *Crystal Structures* (Wiley-Interscience, New York, 1963), Vol. I.
- <sup>67</sup>M. Cardona, in *Atomic Structure and Properties of Solids*, edited by E. Burstein (Academic, New York, 1972), p. 514.
- <sup>68</sup>D. D. Sell, in Ref. 28, p. 800.
- <sup>69</sup>D. E. Aspnes, C. G. Olson, and D. W. Lynch, *Phys. Rev. B* **12**, 2527 (1975).
- <sup>70</sup>M. Chandrasekhar and F. H. Pollak, *Phys. Rev. B* **15**, 2127 (1977).
- <sup>71</sup>D. L. Camphausen, G. A. N. Connell, and W. Paul, *Phys. Rev. Lett.* **26**, 184 (1971).
- <sup>72</sup>C. J. Hwang, *J. Appl. Phys.* **40**, 3731 (1969).
- <sup>73</sup>D. E. Aspnes, C. G. Olson, and D. W. Lynch, in Ref. 42, p. 1000.
- <sup>74</sup>D. E. Aspnes, C. G. Olson, and D. W. Lynch, *Phys. Rev. B* **14**, 2534 (1976).
- <sup>75</sup>F. Bassani and G. Pastori Parravicini, *Electronic States and Optical Transitions in Solids* (Pergamon, Oxford, 1974), Chap. 7.
- <sup>76</sup>R. A. Faulkner, *Phys. Rev.* **175**, 991 (1968).